Electronic Supplementary Material (ESI) for Sensors & Diagnostics.

Supporting Information

Multi-Target Amyloid Probing and Inhibition Using Basic Orange Fluorescence

Yijing Tang[1], Dong Zhang[1], Xiong Gong[2], and Jie Zheng[1*]

[1]Department of Chemical, Biomolecular, and Corrosion Engineering
The University of Akron, Ohio, USA

[2]School of Polymer Science and Polymer Engineering
The University of Akron, Ohio, USA

* Corresponding author: zhengj@uakron.edu

Table S1. Comparison of typical amyloid probes and inhibitors in terms of their K_D value and relative inhibited fibrillization rate

		Entry	Detectors/ Modulators	Target	Binding affinity/Sensitivity (μM)	Inhibition rate (%)	Ref.
Single function-detectors	Single-targeted	1	PicoGreen	insulin	~38.5	-	[1]
		2	stryl-11	insulin	20	-	[2]
		3	Thienoquinoxaline	Aβ	0.077	-	[3]
		4	styryl-quinoxaline (SQ)	Aβ	0.294	-	[3]
		5	L1	Aβ	-	-	[4]
		6	L2	Aβ	-	-	[4]
		7	L3	Aβ	-	-	[4]
		8	Mu1	Aβ	90.91	-	[5]
		9	4b	Aβ	0.0085	-	[6]
		10	ANCA	Aβ	1.4-13.8 (6)	-	[7]
	Multi-targeted	11	Thioflavin T (ThT)	Aβ, hIAPP, hCT, α-syn, etc	~0.58	-	[8,9]
		12	1-anilino-8-naphthalene sulfonate (ANS)	Aβ, hIAPP, hCT, α-syn, etc	-	-	[8]
		13	Benzothiazole aniline (BTA)	Aβ, tau	~0.02	-	[10]
		14	auramine-O (AuO)	BSA, insulin	~1.12	-	[11,12]
		15	PD-NA	Aβ, HEWL	-	-	[13]
		16	PD-NA-TEG	Aβ, HEWL	-	-	[13]
		17	TPE-TPP	Aβ, α-syn, α-LA, HEWL, κ-casein, D76Nβ2m, αB-Crystallin	4.36-8.93	-	[14-16]
Single function-inhibitor	Single-targeted	18	melatonin	hIAPP	-	27	[17]
		19	fisetin	hIAPP	-	23	[17]
		20	azadirachtin	hIAPP	-	~100	[18]
		21	organofluorine	Aβ	-	20-96	[19]
		22	Glyburide	hIAPP	-	47	[20]
		23	repaglinide	hIAPP	-	49	[20]
		24	troglitazone	hIAPP	-	90	[20]

	Multi-targeted	25	EGCG	Aβ, α-syn, tau, TTR, Htt, hCT, hIAPP	-	77-100	21-24
		26	Genistein	Aβ, hIAPP	-	40-63	25
		27	Resveratrol	Aβ, hIAPP	-	88	26
		28	Vitamin k3	HEWL, Aβ	-	77-81	27
		29	morin	Aβ, hIAPP, insulin	-	~100	28-30
		30	quercetin	Aβ, hIAPP, α-syn, tau	-	~100	28,31-33
		31	myricetin	Aβ, hIAPP, α-syn, tau	-	~100	28,34-36
		32	rutin	Aβ, hIAPP	-	~100	37-39
		33	curcumin	Aβ,hIAPP, α-syn, PrP, TTR	-	~100	23,40-44
		34	silibinin	Aβ, hIAPP	-	49-70	20,45
		35	caffeine	Aβ, hIAPP	-	28	46,47
Dual function-detectors and modulators	Single-targeted	36	BSPOTPE	Aβ	-	~100	48
	Multi-targeted	37	Congo red	Aβ, hIAPP, hCT, α-syn, etc	0.1-1.1	-	49,50
		38	Basic orange 21 (BO21)	Aβ, hIAPP, hCT, α-syn	0.015-0.24	~100	51 This work

Table S2. Summary of fluorescence spectroscopic titration

	Linear range (μM)	Linear function	R^2	K_D (nM)
mAβ-BO21	0.625-40	y = 0.3853x + 0.013	0.9502	34
oAβ-BO21	2.5-40	y = 0.4546x + 0.0067	0.9868	15
fAβ-BO21	0.625-40	y = 0.0682x + 0.0095	0.9555	139
mhIAPP-BO21	0.625-40	y = 2.029x + 0.094	0.9786	46
ohIAPP-BO21	1.25-40	y = 0.1771x + 0.0032	0.9994	18
fhIAPP-BO21	2.5-40	y = 0.0539x + 0.0062	0.9742	115
mhCT-BO21	0.625-40	y = 0.1786x + 0.0051	0.9945	29
ohCT-BO21	5-40	y = 0.0832x + 0.003	0.9935	36
fhCT-BO21	2.5-40	y = 0.4642x + 0.1113	0.9810	240

Table S3. Detection limits of BO21 and ThT for different amyloid peptides

	Aβ-BO21	hIAPP-BO21	hCT-BO21	Aβ-ThT	hIAPP-ThT	hCT-ThT
δ	5.512	9.247	9.851	32.94	77.18	116.8
K (μM^{-1})	111.8	142.2	110	185.3	577.5	127.5
DL (μM)	0.1479	0.1951	0.2687	0.5333	0.4009	2.7482
R^2	0.9852	0.9745	0.9528	0.8365	0.9005	0.1616

The detection limits (DL) were estimated based on the 3δ/k method.

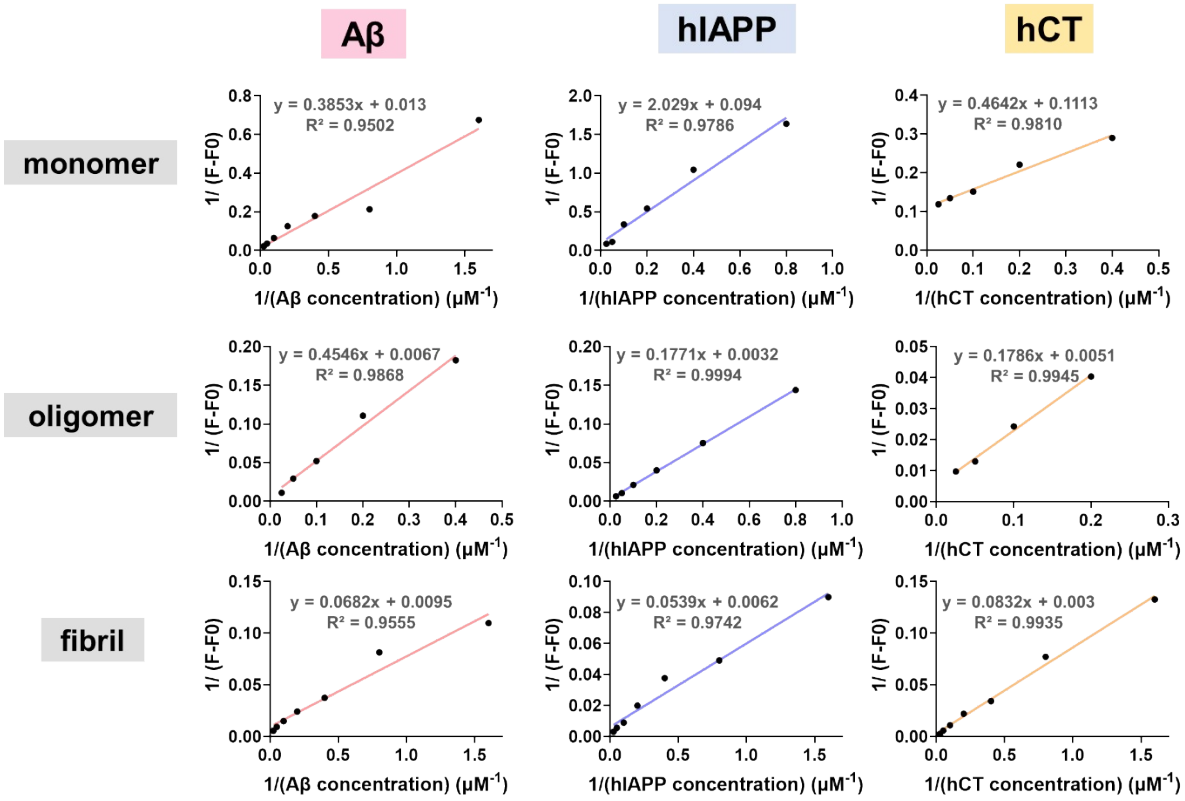

Figure S1. Linear fitting analysis of fluorescence spectroscopic titration shown in **Fig. 3a** using $1/(Ft- F0)=1/(Fmax-F0) +1/((Fmax-F0)\cdot KD\cdot[X])$. 1 μM BO21 was added as the increased concentrations (0-40 μM) of monomeric (1st row), oligomeric (2nd row) and fibrillar (3rd row) aggregates of Aβ (1st column), hIAPP (2nd column), and hCT (3rd column) under excitation of 470 nm.

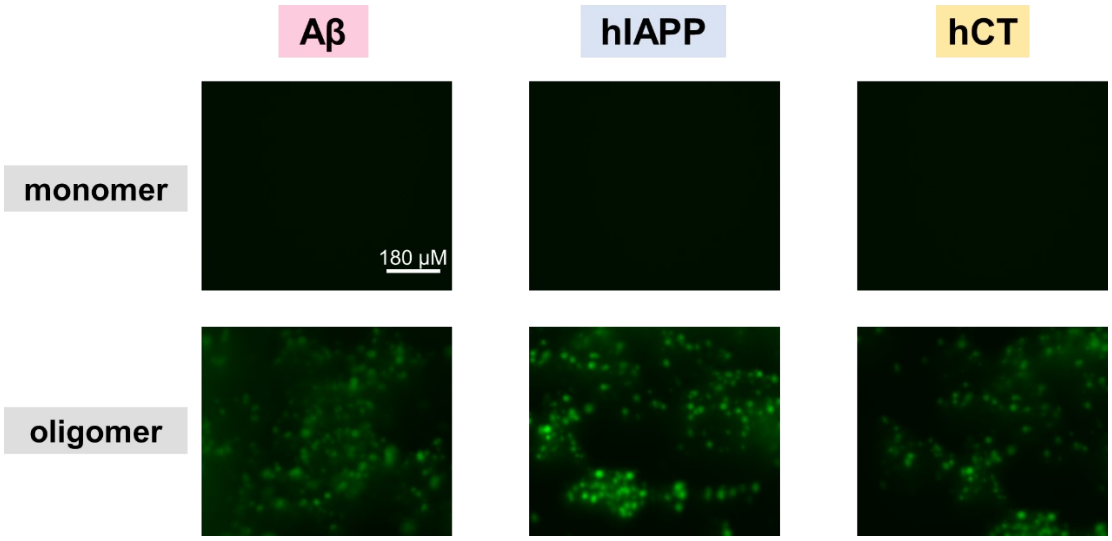

Figure S2. Fluorescence image of amyloid monomers (1st row) and oligomers (2nd row) stained by BO21.

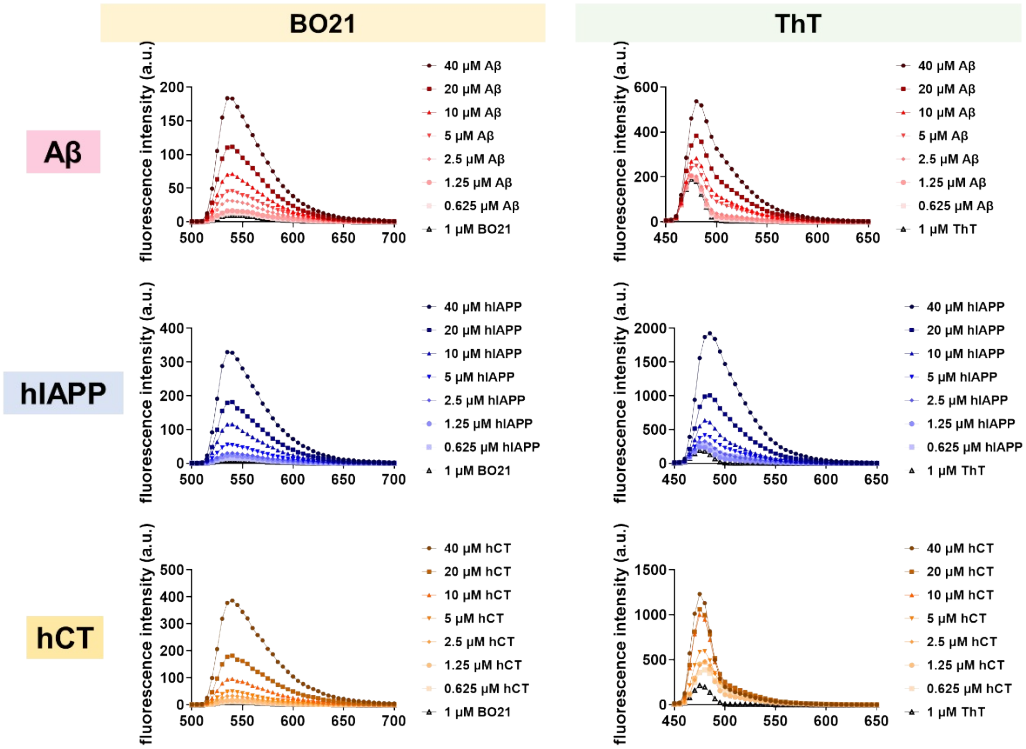

Figure S3. Fluorescence spectra of 1 μM BO21 (1st column) and ThT (2nd column) in the presence (colored) and absence (black) of fibrillar aggregates of Aβ (1st raw), hIAPP (2nd raw), and hCT (3rd raw).

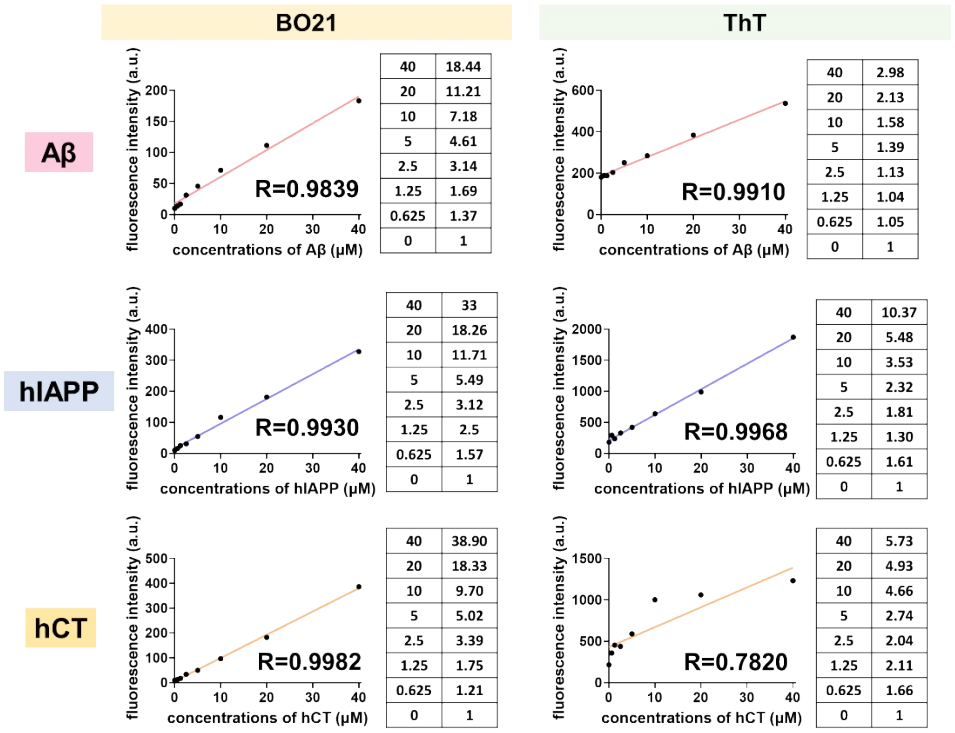

Figure S4. Linear fitting analysis of fluorescence intensity and correasponding signal/noise ratio of using 1 μM BO21 (1st column) and ThT (2nd column) as probe to detect increasing concentrations (0-40 μM) of fibrillar aggregates of Aβ (1st raw), hIAPP (2nd raw), and hCT (3rd raw) under excitation of 470 nm.

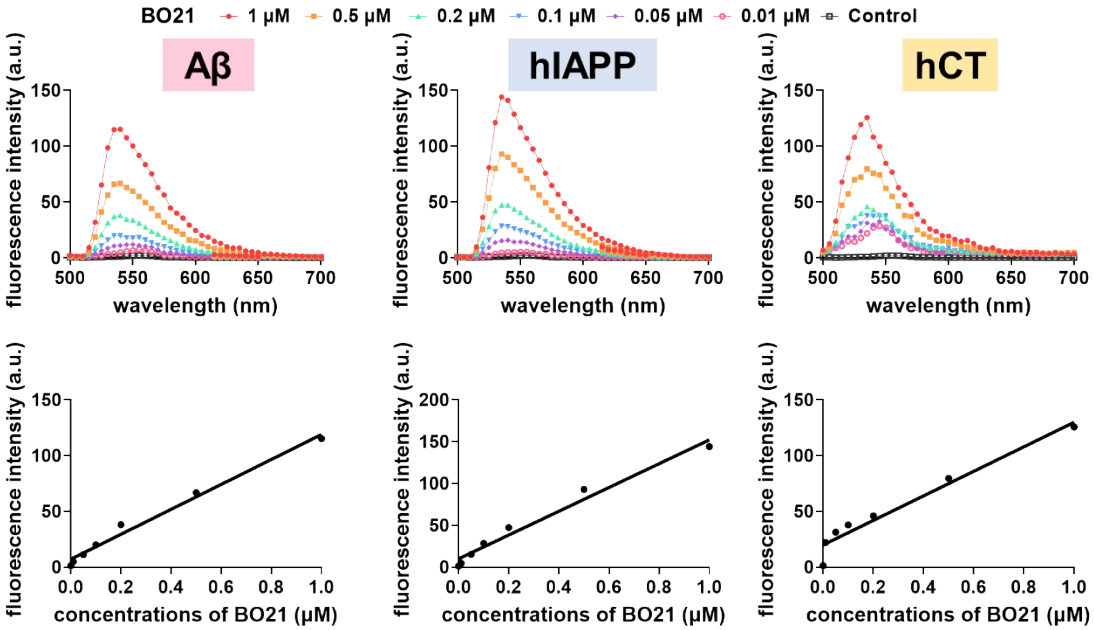

Figure S5. The fluorescence spectrum (1st column) and corresponding linear fitting analysis (2nd column) of 20 μM Aβ (1st column), hIAPP (2nd column), and hCT (3rd column) by stepwise addition of BO21 (0.01 to 1 μM) in PBS buffer (pH = 7.4). λex = 470 nm.

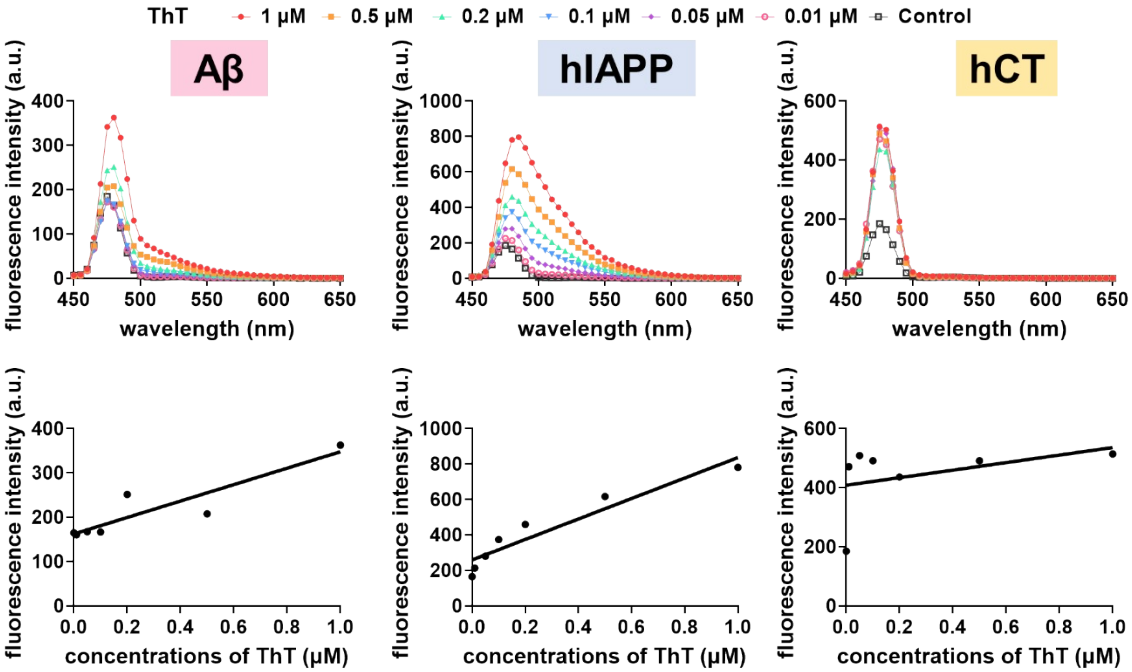

Figure S6. The fluorescence spectrum (1st column) and corresponding linear fitting analysis (2nd column) of 20 μM Aβ (1st column), hIAPP (2nd column), and hCT (3rd column) by stepwise addition of ThT (0.01 to 1 μM) in PBS buffer (pH = 7.4). λex = 450 nm.

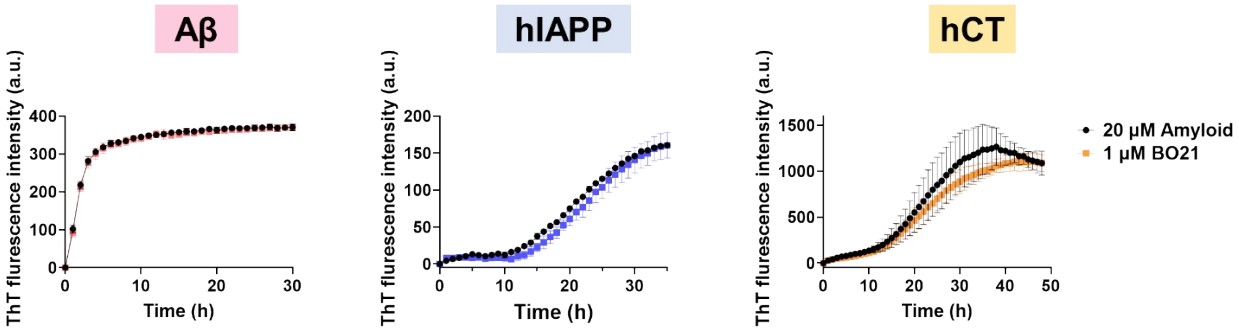

Figure S7. Time-dependent ThT fluorescence curves to monitor the aggregation kinetics of 20 μM pure amyloid peptides of Aβ, hIAPP, and hCT with and without 1 μM BO21.

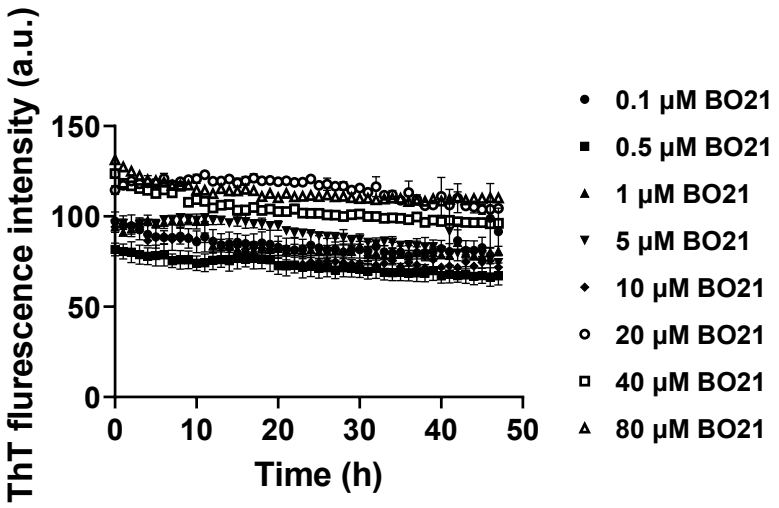

Figure S8. Time-dependent ThT fluorescence curves to monitor the aggregation kinetics of pure BO21 at different concentrations of 0.1-80 μM.

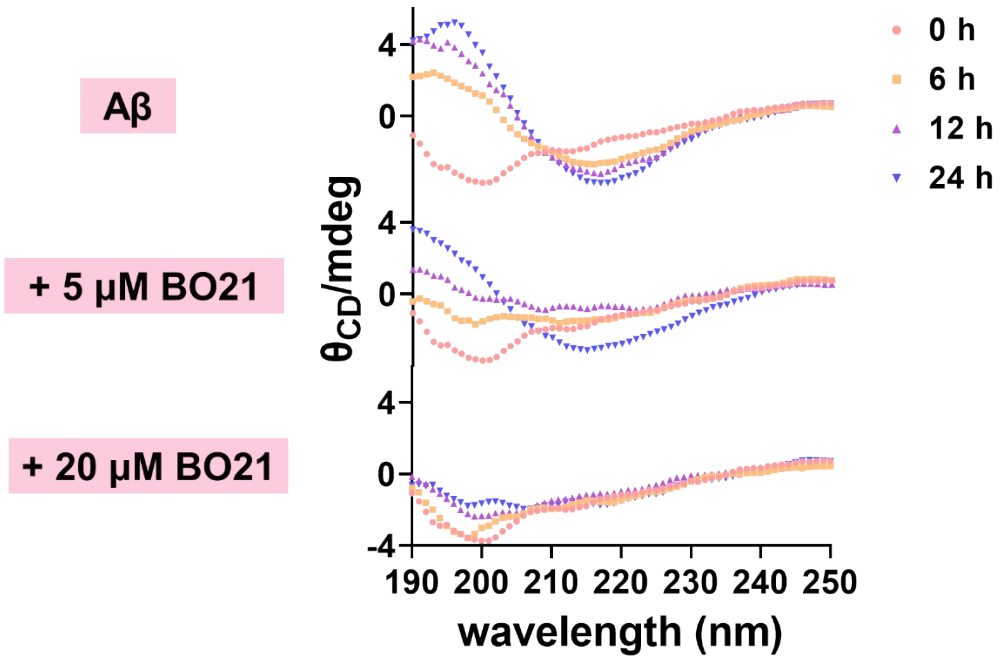

Figure S9. Time-dependent circular dichroism spectra for monitoring the secondary structure changes by adding 5-20 μM BO21 to freshly prepared Aβ.

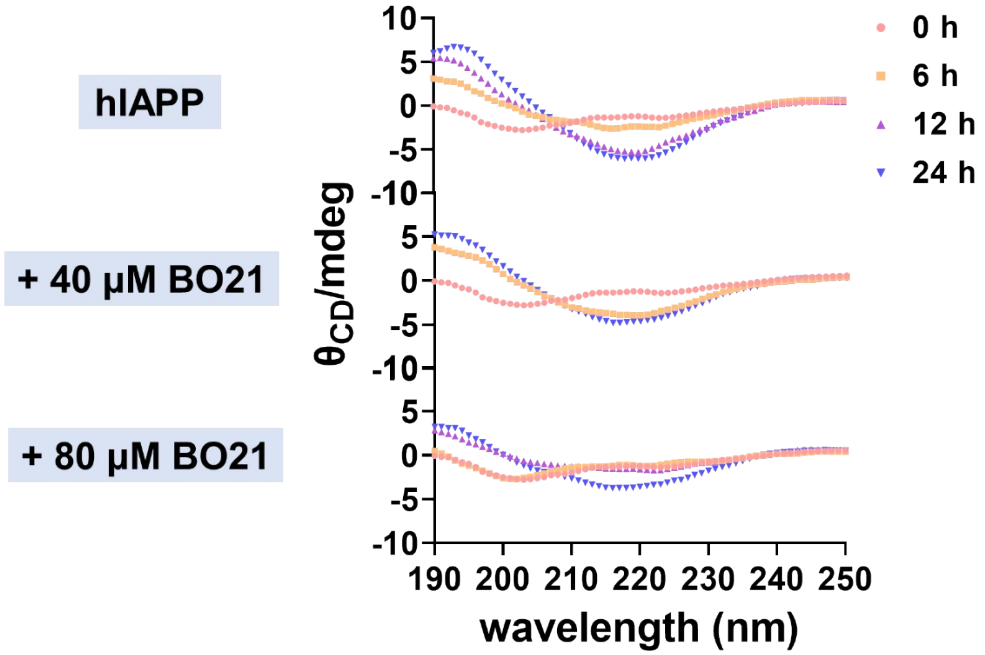

Figure S10. Time-dependent circular dichroism spectra for monitoring the secondary structure changes by adding 20-80 μM BO21 to freshly prepared hIAPP.

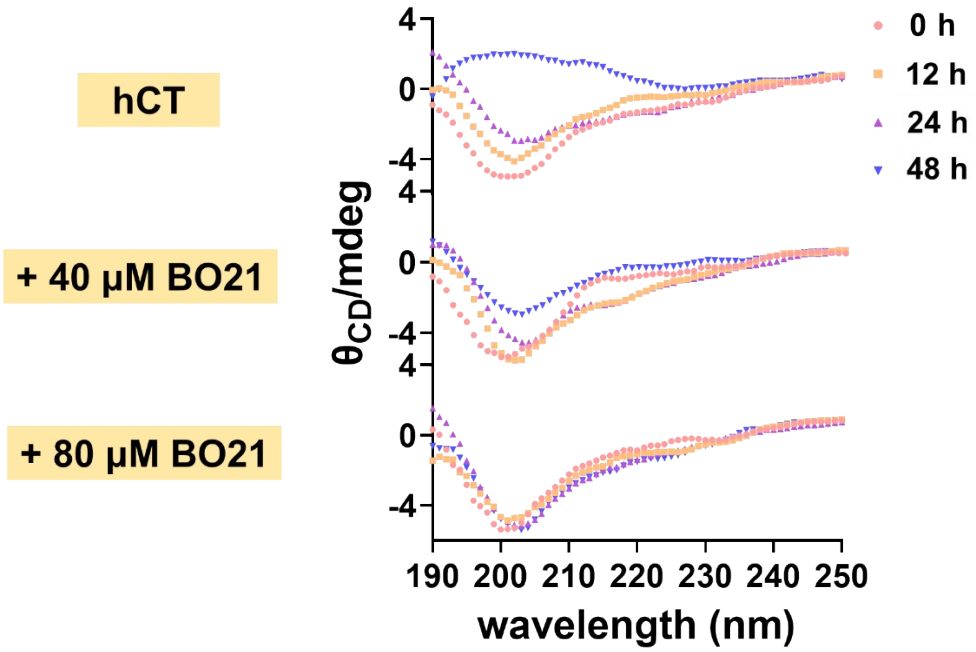

Figure S11. Time-dependent circular dichroism spectra for monitoring the secondary structure changes by adding 20-80 μM BO21 to freshly prepared hCT.

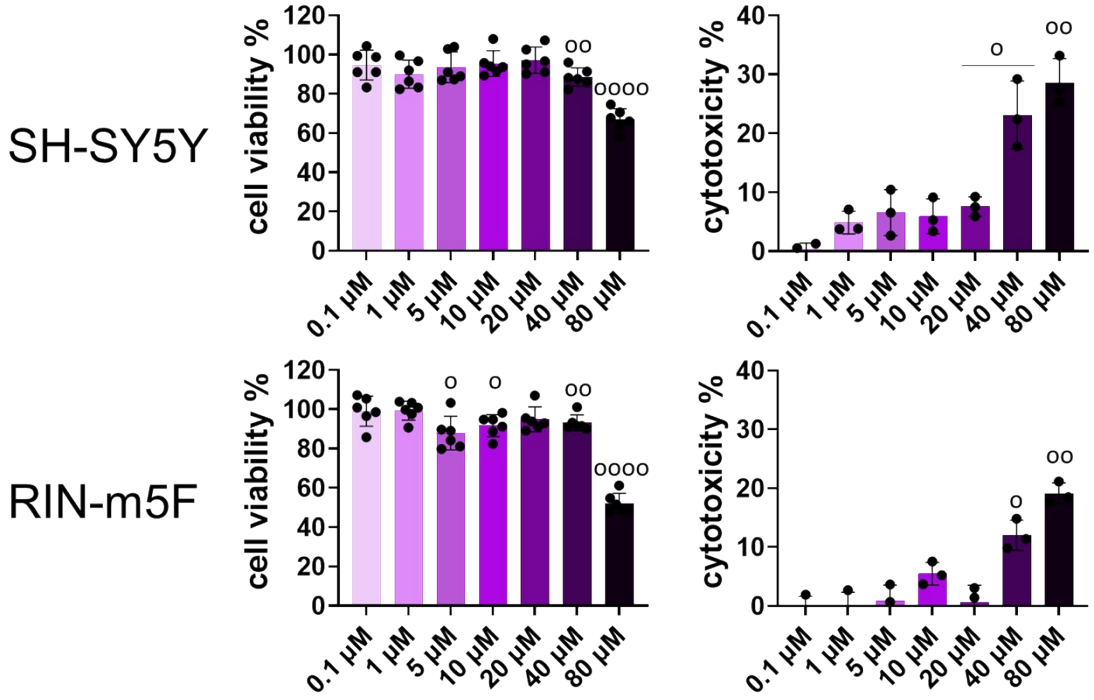

Figure S12. MTT reduction assay for cell viability (1st column) and LDH activity assay for cytotoxicity (2nd column) in the presence of different concentrations of BO21 from 0.1 to 80 µM. t-test was used for data analysis for cells treated with amyloids relative to untreated cell groups (n>3). (°p < 0.05, °°p <0.01, °°°p <0.005, °°°°p <0.001).

Reference

(1) Mora, A. K.; Singh, P. K.; Patro, B. S.; Nath, S. PicoGreen: a better amyloid probe than Thioflavin-T. *Chemical Communications* **2016,** *52* (82), 12163.

(2) Mudliar, N. H.; Singh, P. K. A molecular rotor-based turn-on sensor probe for amyloid fibrils in the extreme near-infrared region. *Chemical Communications* **2019,** *55* (27), 3907.

(3) Benzeid, H.; Mothes, E.; Essassi, E. M.; Faller, P.; Pratviel, G. A thienoquinoxaline and a styryl-quinoxaline as new fluorescent probes for amyloid-β fibrils. *Comptes Rendus Chimie* **2012,** *15* (1), 79.

(4) Dyrager, C.; Vieira, R. P.; Nyström, S.; Nilsson, K. P. R.; Storr, T. Synthesis and evaluation of benzothiazole-triazole and benzothiadiazole-triazole scaffolds as potential molecular probes for amyloid-β aggregation. *New Journal of Chemistry* **2017,** *41* (4), 1566.

(5) Mu, X.; Wu, F.; Wang, R.; Huang, Z.; Lv, T.; Lu, Y.; Liu, B.; Zhou, X. A cyanine-derived NIR molecular rotor for ratiometric imaging of amyloid-β aggregates. *Sensors Actuators B: Chemical* **2021,** *338*, 129842.

(6) Yue, N.; Fu, H.; Chen, Y.; Gao, X.; Dai, J.; Cui, M. Rational design of molecular rotor-based fluorescent probes with bi-aromatic rings for efficient in vivo detection of amyloid-β plaques in Alzheimer's disease. *European Journal of Medicinal Chemistry* **2022,** *243*, 114715.

(7) Chang, W. M.; Dakanali, M.; Capule, C. C.; Sigurdson, C. J.; Yang, J.; Theodorakis, E. A. ANCA: a family of fluorescent probes that bind and stain amyloid plaques in human tissue. *ACS chemical neuroscience* **2011,** *2* (5), 249.

(8) Sulatsky, M.; Sulatskaya, A.; Povarova, O.; Antifeeva, I. A.; Kuznetsova, I.; Turoverov, K. Effect of the fluorescent probes ThT and ANS on the mature amyloid fibrils. *Prion* **2020,** *14* (1), 67.

(9) Ghadami, S. A.; Ahadi-Amandi, K.; Khodarahmi, R.; Ghanbari, S.; Adibi, H. Synthesis of benzylidene-indandione derivatives as quantification of amyloid fibrils. *Biophysical chemistry* **2023,** *296*, 106982.

(10) Klunk, W. E.; Wang, Y.; Huang, G.-f.; Debnath, M. L.; Holt, D. P.; Mathis, C. A. Uncharged thioflavin-T derivatives bind to amyloid-beta protein with high affinity and readily enter the brain. *Life sciences* **2001,** *69* (13), 1471.

(11) Mudliar, N. H.; Sadhu, B.; Pettiwala, A. M.; Singh, P. K. Evaluation of an ultrafast molecular rotor, auramine O, as a fluorescent amyloid marker. *The Journal of Physical Chemistry B* **2016,** *120* (40), 10496.

(12) Amdursky, N.; Huppert, D. Auramine-O as a fluorescence marker for the detection of amyloid fibrils. *The Journal of Physical Chemistry B* **2012,** *116* (45), 13389.

(13) Wang, Y.-L.; Fan, C.; Xin, B.; Zhang, J.-P.; Luo, T.; Chen, Z.-Q.; Zhou, Q.-Y.; Yu, Q.; Li, X.-N.; Huang, Z.-L.et al. AIE-based super-resolution imaging probes for β-amyloid plaques in mouse brains. *Materials Chemistry Frontiers* **2018,** *2* (8), 1554.

(14) Leung, C. W. T.; Guo, F.; Hong, Y.; Zhao, E.; Kwok, R. T. K.; Leung, N. L. C.; Chen, S.; Vaikath, N. N.; El-Agnaf, O. M.; Tang, Y. Detection of oligomers and fibrils of α-synuclein by AIEgen with strong fluorescence. *Chemical Communications* **2015,** *51* (10), 1866.

(15) Das, A.; Gupta, A.; Hong, Y.; Carver, J. A.; Maiti, S. A Spectroscopic Marker for Structural Transitions Associated with Amyloid-β Aggregation. *Biochemistry* **2020,** *59* (19), 1813.
(16) Kumar, M.; Hong, Y.; Thorn, D. C.; Ecroyd, H.; Carver, J. A. Monitoring early-stage protein aggregation by an aggregation-induced emission fluorogen. *Analytical chemistry* **2017,** *89* (17), 9322.
(17) Aarabi, M. H.; Mirhashemi, S. M. To estimate effective antiamyloidogenic property of melatonin and fisetin and their actions to destabilize amyloid fibrils. *Pak J Pharm Sci* **2017,** *30* (5), 1589.
(18) Dubey, R.; Patil, K.; Dantu, S. C.; Sardesai, D. M.; Bhatia, P.; Malik, N.; Acharya, J. D.; Sarkar, S.; Ghosh, S.; Chakrabarti, R. Azadirachtin inhibits amyloid formation, disaggregates pre-formed fibrils and protects pancreatic β-cells from human islet amyloid polypeptide/amylin-induced cytotoxicity. *Biochemical Journal* **2019,** *476* (5), 889.
(19) Török, M.; Abid, M.; Mhadgut, S. C.; Török, B. Organofluorine inhibitors of amyloid fibrillogenesis. *Biochemistry* **2006,** *45* (16), 5377.
(20) Fortin, J. S.; Benoit-Biancamano, M.-O. In vitro evaluation of hypoglycemic agents to target human islet amyloid polypeptide: a key protein involved in amyloid deposition and beta-cell loss. *Canadian journal of diabetes* **2015,** *39* (5), 373.
(21) Xu, Z.-X.; Zhang, Q.; Ma, G.-L.; Chen, C.-H.; He, Y.-M.; Xu, L.-H.; Zhang, Y.; Zhou, G.-R.; Li, Z.-H.; Yang, H.-J. Influence of aluminium and EGCG on fibrillation and aggregation of human islet amyloid polypeptide. *Journal of diabetes research* **2016,** *2016*.
(22) Ehrnhoefer, D. E.; Duennwald, M.; Markovic, P.; Wacker, J. L.; Engemann, S.; Roark, M.; Legleiter, J.; Marsh, J. L.; Thompson, L. M.; Lindquist, S. Green tea (−)-epigallocatechin-gallate modulates early events in huntingtin misfolding and reduces toxicity in Huntington's disease models. *Human molecular genetics* **2006,** *15* (18), 2743.
(23) Ferreira, N.; Saraiva, M. J.; Almeida, M. R. Natural polyphenols inhibit different steps of the process of transthyretin (TTR) amyloid fibril formation. *FEBS letters* **2011,** *585* (15), 2424.
(24) Wobst, H. J.; Sharma, A.; Diamond, M. I.; Wanker, E. E.; Bieschke, J. The green tea polyphenol (−)-epigallocatechin gallate prevents the aggregation of tau protein into toxic oligomers at substoichiometric ratios. *FEBS letters* **2015,** *589* (1), 77.
(25) Ren, B.; Liu, Y.; Zhang, Y.; Cai, Y.; Gong, X.; Chang, Y.; Xu, L.; Zheng, J. Genistein: a dual inhibitor of both amyloid β and human islet amylin peptides. *ACS chemical neuroscience* **2018,** *9* (5), 1215.
(26) Mishra, R.; Sellin, D.; Radovan, D.; Gohlke, A.; Winter, R. Inhibiting islet amyloid polypeptide fibril formation by the red wine compound resveratrol. *ChemBioChem* **2009,** *10* (3), 445.
(27) Alam, P.; Chaturvedi, S. K.; Siddiqi, M. K.; Rajpoot, R. K.; Ajmal, M. R.; Zaman, M.; Khan, R. H. Vitamin k3 inhibits protein aggregation: implication in the treatment of amyloid diseases. *Scientific reports* **2016,** *6* (1), 1.
(28) Ono, K.; Yoshiike, Y.; Takashima, A.; Hasegawa, K.; Naiki, H.; Yamada, M. Potent anti-amyloidogenic and fibril-destabilizing effects of polyphenols in vitro: implications for the prevention and therapeutics of Alzheimer's disease. *Journal of neurochemistry* **2003,** *87* (1), 172.
(29) Noor, H.; Cao, P.; Raleigh, D. P. Morin hydrate inhibits amyloid formation by islet amyloid polypeptide and disaggregates amyloid fibers. *Protein Science* **2012,** *21* (3), 373.

(30) Patel, P.; Parmar, K.; Das, M. Inhibition of insulin amyloid fibrillation by Morin hydrate. *International journal of biological macromolecules* **2018,** *108*, 225.
(31) López, L. C.; Varea, O.; Navarro, S.; Carrodeguas, J. A.; Sanchez de Groot, N.; Ventura, S.; Sancho, J. Benzbromarone, quercetin, and folic acid inhibit amylin aggregation. *International journal of molecular sciences* **2016,** *17* (6), 964.
(32) Zhu, M.; Han, S.; Fink, A. L. Oxidized quercetin inhibits α-synuclein fibrillization. *Biochimica et Biophysica Acta (BBA)-General Subjects* **2013,** *1830* (4), 2872.
(33) Kumar, S.; Krishnakumar, V. G.; Morya, V.; Gupta, S.; Datta, B. Nanobiocatalyst facilitated aglycosidic quercetin as a potent inhibitor of tau protein aggregation. *International journal of biological macromolecules* **2019,** *138*, 168.
(34) Aarabi, M.-H.; Mirhashemi, S. M. The role of two natural flavonoids on human amylin aggregation. *African Journal of Pharmacy and Pharmacology* **2012,** *6* (31), 2374.
(35) Ono, K.; Yamada, M. Antioxidant compounds have potent anti-fibrillogenic and fibril-destabilizing effects for α-synuclein fibrils in vitro. *Journal of neurochemistry* **2006,** *97* (1), 105.
(36) Taniguchi, S.; Suzuki, N.; Masuda, M.; Hisanaga, S.-i.; Iwatsubo, T.; Goedert, M.; Hasegawa, M. Inhibition of heparin-induced tau filament formation by phenothiazines, polyphenols, and porphyrins. *Journal of Biological Chemistry* **2005,** *280* (9), 7614.
(37) Aitken, J. F.; Loomes, K. M.; Riba-Garcia, I.; Unwin, R. D.; Prijic, G.; Phillips, A. S.; Phillips, A. R.; Wu, D.; Poppitt, S. D.; Ding, K. Rutin suppresses human-amylin/hIAPP misfolding and oligomer formation in-vitro, and ameliorates diabetes and its impacts in human-amylin/hIAPP transgenic mice. *Biochemical and biophysical research communications* **2017,** *482* (4), 625.
(38) Yu, X.-L.; Li, Y.-N.; Zhang, H.; Su, Y.-J.; Zhou, W.-W.; Zhang, Z.-P.; Wang, S.-W.; Xu, P.-X.; Wang, Y.-J.; Liu, R.-T. Rutin inhibits amylin-induced neurocytotoxicity and oxidative stress. *Food & Function* **2015,** *6* (10), 3296.
(39) Wang, S.-w.; Wang, Y.-J.; Su, Y.-j.; Zhou, W.-w.; Yang, S.-g.; Zhang, R.; Zhao, M.; Li, Y.-n.; Zhang, Z.-p.; Zhan, D.-w. Rutin inhibits β-amyloid aggregation and cytotoxicity, attenuates oxidative stress, and decreases the production of nitric oxide and proinflammatory cytokines. *Neurotoxicology* **2012,** *33* (3), 482.
(40) Daval, M.; Bedrood, S.; Gurlo, T.; Huang, C.-J.; Costes, S.; Butler, P. C.; Langen, R. The effect of curcumin on human islet amyloid polypeptide misfolding and toxicity. *Amyloid* **2010,** *17* (3-4), 118.
(41) Sparks, S.; Liu, G.; Robbins, K. J.; Lazo, N. D. Curcumin modulates the self-assembly of the islet amyloid polypeptide by disassembling α-helix. *Biochemical and biophysical research communications* **2012,** *422* (4), 551.
(42) Yang, F.; Lim, G. P.; Begum, A. N.; Ubeda, O. J.; Simmons, M. R.; Ambegaokar, S. S.; Chen, P. P.; Kayed, R.; Glabe, C. G.; Frautschy, S. A. Curcumin inhibits formation of amyloid β oligomers and fibrils, binds plaques, and reduces amyloid in vivo. *Journal of Biological Chemistry* **2005,** *280* (7), 5892.
(43) Pandey, N.; Strider, J.; Nolan, W. C.; Yan, S. X.; Galvin, J. E. Curcumin inhibits aggregation of α-synuclein. *Acta neuropathologica* **2008,** *115* (4), 479.
(44) Caughey, B.; Raymond, L. D.; Raymond, G. J.; Maxson, L.; Silveira, J.; Baron, G. S. Inhibition of protease-resistant prion protein accumulation in vitro by curcumin. *Journal of virology* **2003,** *77* (9), 5499.

(45) Yin, F.; Liu, J.; Ji, X.; Wang, Y.; Zidichouski, J.; Zhang, J. Silibinin: A novel inhibitor of Aβ aggregation. *Neurochemistry international* **2011,** *58* (3), 399.
(46) Cheng, B.; Liu, X.; Gong, H.; Huang, L.; Chen, H.; Zhang, X.; Li, C.; Yang, M.; Ma, B.; Jiao, L. Coffee components inhibit amyloid formation of human islet amyloid polypeptide in vitro: possible link between coffee consumption and diabetes mellitus. *Journal of agricultural food chemistry* **2011,** *59* (24), 13147.
(47) Sharma, B.; Paul, S. Action of caffeine as an amyloid inhibitor in the aggregation of Aβ16–22 peptides. *The Journal of Physical Chemistry B* **2016,** *120* (34), 9019.
(48) Hong, Y.; Meng, L.; Chen, S.; Leung, C. W. T.; Da, L.-T.; Faisal, M.; Silva, D.-A.; Liu, J.; Lam, J. W. Y.; Huang, X. Monitoring and inhibition of insulin fibrillation by a small organic fluorogen with aggregation-induced emission characteristics. *Journal of the American Chemical Society* **2012,** *134* (3), 1680.
(49) Groenning, M. Binding mode of Thioflavin T and other molecular probes in the context of amyloid fibrils—current status. *Journal of chemical biology* **2010,** *3*, 1.
(50) Lorenzo, A.; Yankner, B. A. Beta-amyloid neurotoxicity requires fibril formation and is inhibited by congo red. *Proceedings of the National Academy of Sciences* **1994,** *91* (25), 12243.
(51) Pandey, S. P.; Singh, P. K. Basic Orange 21: a molecular rotor probe for fluorescence turn-on sensing of amyloid fibrils. *Journal of Molecular Liquids* **2020,** *303*, 112618.